

Quantum critical points in tunneling junction of topological superconductor and topological insulator

Zheng-Wei Zuo^{a,b,*}, Da-wei Kang^a, Zhao-Wu Wang^{a,b}, Liben Li^a

^a*School of Physics and Engineering, Henan University of Science and Technology, Luoyang 471003, China*

^b*National Laboratory of Solid State Microstructures, Nanjing University, Nanjing 210093, China*

Abstract

The tunneling junction between one-dimensional topological superconductor and integer (fractional) topological insulator (TI), realized via point contact, is investigated theoretically with bosonization technology and renormalization group methods. For the integer TI case, in a finite range of edge interaction parameter, there is a non-trivial stable fixed point which corresponds to the physical picture that the edge of TI breaks up into two sections at the junction, with one side coupling strongly to the Majorana fermion and exhibiting perfect Andreev reflection, while the other side decouples, exhibiting perfect normal reflection at low energies. This fixed point can be used as a signature of the Majorana fermion and tested by nowadays experiment techniques. For the fractional TI case, the universal low-energy transport properties are described by perfect normal reflection, perfect Andreev reflection, or perfect insulating fixed points dependent on the filling fraction and edge interaction parameter of fractional TI.

Keywords: Majorana fermion, topological insulator, Andreev reflection

1. introduction

Recently, the study of topological superconductors which support Majorana fermion excitations has been a focus of theoretical and experimental studies in condensed matter physics[1, 2, 3]. Majorana fermions being their own anti-particles have exotic non-Abelian braiding statistics and great potential in the applications of fault-tolerant topological quantum computation[4]. There are many proposals which allow us to engineer topological superconductor (TSC), based on proximity coupling to *s*-wave superconductors. These include topological insulators[5, 6], semiconductor quantum wires[7, 8], and chains of magnetic adatoms[9, 10, 11, 12, 13]. Among these proposals, the most promising

*Corresponding author. Tel:+8618337991815
Email address: zuozw@163.com (Zheng-Wei Zuo)

candidate for the experimental realization is the semiconductor quantum wires proposal[1, 14]. The experimental evidences of Majorana fermions have been shown in spin-orbit coupled quantum wire model[15, 16, 17]. All other proposals are being actively pursued[18, 19].

Because of these intrinsically fascinating of Majorana fermions, there are many interesting transport properties and critical points when TSC couples to other materials [20, 21, 22, 23, 24, 25, 26, 27, 28, 29, 30, 31, 32, 33]. A junction between a TSC and a Fermi lead (or interacting lead) is predicted to exhibit perfect Andreev reflection at low energies[20, 23]. Further, a novel type of quantum frustration and quantum critical points appear at low energies when one-dimensional (1D) TSC couples to two interacting leads or an interacting lead with two channels[23, 24, 25]. At this critical point, the perfect Andreev reflection occurs in one interacting lead (one channel) and perfect normal reflection in the other. The tunneling junction between a TSC with chiral Majorana liquid at the edge and a helical Luttinger liquid is studied[28], the main conclusion of which is that at low energies, the helical Luttinger liquids is cut into two separated half wires by backscattering potential and the tunneling between the Majorana liquid and the helical Luttinger liquid is forbidden. The perfect Andreev transmission (the reflected hole goes into a different lead from where the electron arrived) can occur when the edge of topological insulator (TI) contacts with a Kramers pair of Majorana fermions in TSC[33].

Usually, the quantum wires with electron-electron interaction are described by Luttinger liquids theory[34, 35] and the low-energy physics of the tunneling junctions between TSC and interacting quantum wires are analyzed by renormalization group method[23, 24, 25, 26, 27, 28, 29, 30, 31]. These interacting quantum wires are topological trivial systems. In contrast, the interplay of the TSC and other topological matters may result in novel and interesting transport properties. Recently, we have studied the point contact tunneling junction between 1D TSC and single-channel quantum Hall (QH) liquids[36]. For the $\nu = 1$ integer QH liquid, the perfect Andreev reflection with quantized zero-bias tunneling conductance $2e^2/h$ is predicted to occur at zero temperature and voltage, which is caused by Majorana fermion tunneling not by the Cooper-pair tunneling. The quantized conductance can serve as a definitive fingerprint of a Majorana fermion. However, for the Laughlin fractional QH liquid cases, the universal low-energy transport is governed by the perfect normal reflection fixed point with vanishing zero-bias tunneling conductance.

The edges states of two-dimensional (2D) integer TI, known as helical liquid, are topologically protected by time-reversal symmetry. The localized Majorana modes emerge at interface of superconductor-ferromagnet junction on the edge of 2D TI[6, 37]. The different geometries of TSC coupling with the edge of 2D TI have been investigated[28, 32, 33]. The fractional TI [38, 39, 40, 41, 42, 43], which is the strongly interacting version of 2D TI, can be regarded as the generalization of the fractional QH liquids to time-reversal-invariant systems. The simplest case of a fractional TI consists of two decoupled copies of a Laughlin fractional QH states with opposite spin polarizations. The parafermions (fractionalizing Majorana fermions) can be obtained at the interface between a SC

and a ferromagnet along the edge of fractional TI[44, 45, 46, 47]. Due to these intriguing and exotic properties, it is of both theoretical and practical interest to investigate the transport properties of junction between the TSC and integer (fractional) TI.

The content of the paper is organized as follows. In Sec. 2, using bosonization technology and renormalization group methods, we firstly research the tunneling transport signatures of 1D TSC and integer TI. In a finite range of edge interaction parameter, the edge of TI breaks up into two sections at the junction, with one side having perfect Andreev reflection due to Majorana fermion tunneling, while the other side decouples, having perfect normal reflection. This physical picture of our setup can be tested by present experimental techniques. Next, we calculate the phase diagram of the fractional TI case. In Sec. 3, we make discussions and concluding remarks.

2. Theory and Discussion

In this section, we consider the point contact tunneling junction of 1D TSC and filling fraction $\nu = 1/m$ (m is an odd integer) fractional TI, as shown in Fig. 1. When $m = 1$, the fractional TI degenerates into 2D topological insulator. Next, we will use TI to denote the integer and fractional TI, except where confusion might result from these abbreviations.

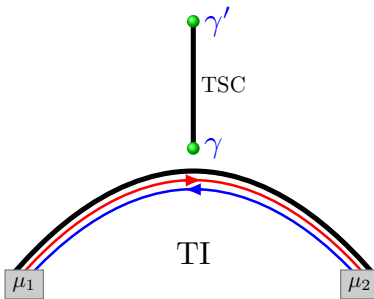


Figure 1: Schematic illustration of the tunneling junction between TSC and TI. The edge of TI can be described in terms of two bosonic fields ϕ_α . The 1D TSC is characterized by the Majorana fermions γ and γ' .

The 1D TSC is characterized by the two Majorana fermions γ and γ' at end points, which can be obtained by a spin-orbit coupled quantum wire subjected to a magnetic field and proximate to an s-wave superconductor[7, 8]. We assume all the important energy scales are smaller than the superconducting energy gap and the 1D TSC is sufficiently long so that Majorana fermion γ' do not couple to electrons in the TI. The fractional TI we analyze consists of two coupled fractional QH states, in which electrons of spin up form a Laughlin fractional QH states with filling fraction $\nu_\uparrow = 1/m$ and electrons of spin down form a Laughlin fractional QH states with filling fraction $\nu_\downarrow = -1/m$. The edge states of the TI are helical Luttinger liquid and the top edge of TI connects leads μ_1

and μ_2 . Here, we label the right and left sides of junction by $x > 0$ and $x < 0$ respectively, and assume that the two leads are infinitely far away.

The Hamiltonian of the tunneling junction can be expressed as

$$H = H_0 + H_T \quad (1)$$

where H_0 is the Hamiltonian of TI edge theory and H_T tunneling Hamiltonian.

Firstly, we discuss the edge theories (helical Luttinger liquids) of integer TI[48, 49] and fractional TI[39, 40, 50]. Here, we express these theories within a unified framework. When $m = 1$, these reduce to integer TI case. The edges of TI can be described by two chiral bosonic quantum fields ϕ_α and the density operators are

$$\rho_\alpha = \frac{1}{2\pi} \partial_x \phi_\alpha \quad (2)$$

where $\alpha = R$ (right-mover with spin up), L (left-mover with spin down).

The boson fields ϕ_α satisfy the Kac-Moody commutation relations

$$[\phi_\alpha(x), \phi_\beta(x')] = (\sigma_z)_{\alpha\beta} \frac{i\pi}{m} \text{sgn}(x - x') \quad (3)$$

Because of the time-reversal symmetry, the Hamiltonian of the edge of the TI is

$$H_0 = \int dx [\pi m v_F (\rho_R^2 + \rho_L^2) + 2g_2 \rho_R \rho_L + g_4 (\rho_R^2 + \rho_L^2)] \quad (4)$$

where g_2 and g_4 are the amplitudes for dispersion and forward scattering processes.

To simplify our derivation, we introduce the fields

$$\varphi = \frac{1}{2} (\phi_R + \phi_L), \theta = \frac{1}{2} (\phi_R - \phi_L) \quad (5)$$

According to the theory of Luttinger liquids[34, 35], we can express the Hamiltonian as

$$H_0 = \frac{mu}{2\pi} \int dx \left[K (\partial_x \theta)^2 + \frac{1}{K} (\partial_x \varphi)^2 \right] \quad (6)$$

with

$$K = \sqrt{\frac{\pi m v_F + g_4 - g_2}{\pi m v_F + g_4 + g_2}}$$

$$u = \sqrt{\left(1 + \frac{g_4}{\pi m v_F}\right)^2 - \left(\frac{g_2}{\pi m v_F}\right)^2}$$

where $K < 1$ ($K > 1$) for repulsive (attractive) edge interaction, and $K = 1$ corresponds to a noninteracting edge. For the noninteracting edge, the fractional TI can be substituted by a simple electron-hole bilayer where the two layers are in a Laughlin fractional QH states with filling fraction $\nu = \pm 1/m$.

The electron creation operators can be expressed as

$$\Psi_\alpha^\dagger(x) = \Gamma_\alpha e^{im(\sigma_z)_{\alpha\alpha}\phi_\alpha} \quad (7)$$

with Γ_α the Klein factor that is used to ensure the correct anti-commutation relations between different fermion species and obey the following commutation relations.

$$\Gamma_\alpha^\dagger = \Gamma_\alpha, \{\Gamma_\alpha, \Gamma_\beta\} = 2\delta_{\alpha\beta}, \{\Gamma_\alpha, \gamma_\beta\} = 0 \quad (8)$$

From the first relation above, we can view Klein factors as additional Majorana fermions, which is important for studying related Majorana fermion models as shown in [51, 52]. The third equation ensure the anti-commutation relations of electrons Ψ_α and Majorana fermion γ .

As regards the various couplings at the point contact, there are three major types of tunneling processes: the Majorana fermion-induced tunneling, the Cooper pairs tunneling, and backscattering of electrons in the helical Luttinger liquid. The tunneling Hamiltonian of our system at $x = 0$ can be expressed as

$$\begin{aligned} H_T = & \gamma \sum_\alpha t_\alpha [\Psi_\alpha - \Psi_\alpha^\dagger] + \Delta [\Psi_R^\dagger \Psi_L^\dagger + H.c] \\ & + u [\Psi_R^\dagger \Psi_L + H.c] \end{aligned} \quad (9)$$

where the first term stands for Majorana fermion coupling to electrons of TI, the second term is the tunneling of Cooper pairs between TSC and TI. The second term Δ is the s -wave Cooper-pair tunneling induced locally in the wire by the superconducting pairing[23, 53], similar to the tunnel junction between conventional superconductor and multicomponent fractional QH liquids[54, 55]. The third term u is the backscattering of electrons in the helical Luttinger liquid. As supposed in Ref. [28], the backscattering of electrons can occur because of the broken time-reversal symmetry by the TSC. For time-reversal invariant TSC, the electrons backscattering is forbidden[33].

After bosonization, the tunneling term becomes

$$\begin{aligned} H_T = & 2i\gamma \sum_\alpha t_\alpha \Gamma_\alpha \cos [m(\varphi(0) \pm \theta(0))] + 2\Delta \sin [2m\theta(0)] \\ & + 2u \sin [2m\varphi(0)] \end{aligned} \quad (10)$$

where the upper (lower) sign is for $\alpha = R (L)$. The first tunneling term factorize into Klein-Majorana interaction and charge sector parts. We can define ordinary fermion $\psi_\alpha = (\gamma + i\Gamma_\alpha)/2$ with $\{\psi_\alpha, \psi_\alpha^\dagger\} = 1$, so

$$i\gamma\Gamma_\alpha = 2\psi_\alpha^\dagger\psi_\alpha - 1 = \pm 1 \quad (11)$$

and we can see that the values correspond to this energy level being occupied and empty. Consequently, the Klein-Majorana fusion procedure can eliminate the Majorana degrees of freedom[51, 52] and simplify our theoretical calculations.

We first assume t_α , Δ and u are weak perturbation and study these fate using perturbative renormalization group (RG) analysis. First, we pass to a

Lagrangian formalism by a Legendre transform of the Hamiltonian and integrate out the bosonic fields in the partition function of the system except at $x = 0$, then obtain a theory defined only at the location of the point contact. Next, the bosonic field $\varphi(\theta)$ are split into slow (s) and fast (f) modes: $\varphi_s(\tau) = \int_{-\Lambda/b}^{\Lambda/b} \frac{d\omega}{2\pi} e^{-i\omega\tau} \varphi(\omega)$ and $\varphi_f(\tau) = \int_{\Lambda/b < |\omega| < \Lambda} \frac{d\omega}{2\pi} e^{-i\omega\tau} \varphi(\omega)$, with Λ as an energy cutoff, $b > 1$ as a scale factor, and $\tau = it$ the Euclidean time. The θ_s and θ_f have a similar definition. Third, we integrate over the fast modes and the new effective action for the slow degrees of freedom can be calculated using cumulant expansion to the lowest-order approximation. Last, the effective action is identical in its structure to the original action hence is renormalizable and the next step is rescaling. In a word, the lowest-order flows for the coupling t_α , Δ , and u are

$$\frac{dt_\alpha}{d \ln b} = t_\alpha \left(1 - \frac{m}{4} \left(K + \frac{1}{K} \right) \right) \quad (12)$$

$$\frac{d\Delta}{d \ln b} = \Delta \left(1 - \frac{m}{K} \right) \quad (13)$$

$$\frac{du}{d \ln b} = u(1 - mK) \quad (14)$$

In what follows, we first analyze the phase diagrams of integer TI coupling to 1D TSC and calculate its transport signatures. Then, the fractional TI case is investigated.

2.1. Topological insulator case

When $m = 1$, our system reduces to the 2D integer TI (quantum spin Hall effect) case. From Eq.(12), we can see that when $2 - \sqrt{3} < K < 2 + \sqrt{3}$, the Majorana fermion coupling to electrons term becomes relevant. For $K > 1$, the Cooper-pair tunneling term becomes relevant (from Eq.13). When $K < 1$, the electrons backscattering is relevant (from Eq.14). So, when $1 < K < 2 + \sqrt{3}$, the Majorana fermion coupling and Cooper-pair tunneling are in competition with each other. For $2 - \sqrt{3} < K < 1$, the Majorana fermion coupling and electrons backscattering are in competition with each other. Thus, the tunneling junction will exhibit fascinating phase diagrams. According to these RG flows of Eqs. (12-14), for $K > \sqrt{3}$, the Cooper-pair tunneling is the dominant scattering process and the low-energy transport is controlled by perfect Andreev reflection fixed point with quantized zero-bias conductance $2e^2/h$. For $K < 1/\sqrt{3}$, the electrons backscattering is most relevant and the system flows to the perfect insulating fixed point at low energies, analogous to the result of Ref. [28]. This fixed point corresponds to the physics picture where the backscattering cuts the edge of TI into two halves (denoted by right R and left L sides) and the conductance between the leads μ_1 and μ_2 is zero. The perfect insulating fixed point in our setup and the fixed point I in Ref. [28] are the same, because the edge in each setup is effectively cut into two separated pieces by electron backscattering at the quantum point contact. There are no currents flowing through the edge of TI and we have two half-infinite helical Luttinger liquids.

Next, we first analyze the stability of the perfect insulating fixed point for $K < 1/\sqrt{3}$, and then research the scattering properties for $1/\sqrt{3} < K < \sqrt{3}$, where the Majorana fermions coupling is most relevant.

2.1.1. Phase diagram

For convenience, we regard the left and right edge parts of 2D TI at $x = 0$ as the leads L_μ and R_μ . To investigate the stability of the perfect insulating fixed point for $K < 1/\sqrt{3}$, we consider the possible perturbations around it. Now, our system is similar to 1D TSC coupling to two interacting leads or one lead with two channels[23, 24, 28], while the differences from our system are that the two leads are the edges of 2D TI and have the same Luttinger interaction parameter K . So, we can use these part conclusion for our setup. Physically, the deviations from this fixed point mean that the single electron transmission between left and right sides at $x = 0$ is allowed. There are other possible perturbation around it such as Majorana fermion tunneling t_β ($\beta = R_\mu, L_\mu$) and Cooper-pair tunneling Δ_β . The single electron transmission λ can be expressed as

$$H_\lambda = \lambda (\Psi^\dagger(0^+) \Psi(0^-) + H.c) \quad (15)$$

Based on the above RG analysis, we can derive the scaling dimensions of t_β , Δ_β , and λ , yielding $D(t_\beta) = 1/(2K)$, $D(\Delta_\beta) = 2/K$, and $D(\lambda) = 1/K$. So, the Cooper-pair tunneling and single electron transmission are irrelevant. However, the Majorana fermion tunneling is relevant for $1/2 < K < 1/\sqrt{3}$ and destabilize the perfect insulating fixed point. We may naively conclude that the Majorana fermion is simultaneously and strongly coupling with the two sides under renormalization and the low-energy transport is controlled by perfect Andreev reflection fixed points in the two sides (label $A \otimes A$). However, this $A \otimes A$ fixed point is unstable, as shown in Ref [24]. First, the $A \otimes A$ quantum critical point occurs only when t_1 and t_2 exactly balance. But, the Majorana fermion has a spin structure[56, 57]. Generally, Majorana fermion γ couples with one side stronger than the other. Second, using the ‘ ϵ -expansion’ techniques[24], we can derive that the bigger tunneling t_β grows under renormalization and the smaller flow to zero. So, the system flows to $A \otimes N$ or $N \otimes A$ fixed points which corresponding to perfect Andreev reflection with quantized zero-bias tunneling conductance $2e^2/h$ in one side and perfect normal reflection with vanishing zero-bias tunneling conductance in the other. Here, we discuss the stability of the $A \otimes N$ or $N \otimes A$ fixed points. For simplicity, we assume the system flows to $A \otimes N$ fixed point where perfect Andreev reflection occurs in left side and perfect normal reflection takes place in the right side. The possible perturbations around this fixed point are that the electrons backscattering $\Psi_R^\dagger(0^-) \Psi_L(0^-) + H.c$ in left side with scaling dimension $2K$, Cooper-pair tunneling $\Psi_R^\dagger(0^+) \Psi_L^\dagger(0^+) + H.c$ in right side with scaling dimension $2/K$, and electrons transmission $\Psi^\dagger(0^+) \Psi(0^-) + H.c$ between the two sides with scaling dimension $(K + 1/K)/2$. All these perturbations are irrelevant. Thus, for $1/2 < K < 1/\sqrt{3}$, the low-energy physics is described by $A \otimes N$ or $N \otimes A$ fixed points where the edge of TI breaks up into two sections at the junction, with one

side coupling strongly to the Majorana mode and exhibiting perfect Andreev reflection, while the other side decouples, exhibiting perfect normal reflection. The illustrative picture of $A \otimes N$ or $N \otimes A$ fixed points is shown in Fig.2. In addition, for $K < 1/2$, the perfect insulating fixed point is stable.

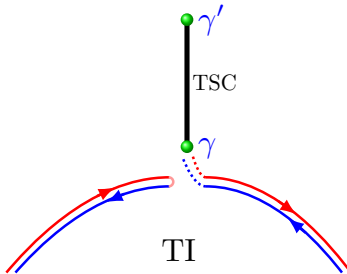


Figure 2: Schematic illustration picture of $A \otimes N$ or $N \otimes A$ fixed points.

Next, we analyze the scattering processes for the region of $1/\sqrt{3} < K < \sqrt{3}$. Now, the Majorana fermions coupling is the leading relevant operator. Under renormalization, the Majorana fermion couples more strongly with the two right and left movers (chiral bosonic fields ϕ_α). This might indicate the system flows toward $A \otimes A$ fixed point. As discussed above, this $A \otimes A$ fixed point is also unstable. The reason is that the critical point $A \otimes A$ needs PT (parity \otimes time reversal) symmetry protecting, while the electrons backscattering $\Psi_R^\dagger \Psi_L + H.c.$ term breaks time reversal symmetry, as shown in the Appendix F in Ref [24]. By way of the ‘ ϵ -expansion’ techniques, we found that the system flows to $A \otimes N$ or $N \otimes A$ fixed points which corresponding to perfect Andreev reflection in one mover and perfect normal reflection in the other. According to the perfect Andreev reflection boundary condition $\Psi_R^\dagger(0^\pm) = -\Psi_L(0^\pm)$, the edge of TI breaks up into two sections at the junction, with one side coupling strongly to the Majorana mode and exhibiting perfect Andreev reflection, while the other side decouples, exhibiting perfect normal reflection. This result is the same as the case for the region of $1/2 < K < 1/\sqrt{3}$. So, the $A \otimes N$ or $N \otimes A$ fixed points are stable for $1/\sqrt{3} < K < \sqrt{3}$. In summary, we can derive the phase diagram of the integer TI case, as shown in table 1. For $K > \sqrt{3}$, the low-energy physics is governed by the perfect Andreev reflection fixed point with Cooper-pair tunneling. For $1/2 < K < \sqrt{3}$, there exist $A \otimes N$ or $N \otimes A$ fixed points where the edge of TI breaks up into two sections at the junction, perfect Andreev reflection with quantized zero-bias tunneling conductance $2e^2/h$ occurs in one side and perfect normal reflection with vanishing zero-bias tunneling conductance occurs in the other. For $K < 1/2$, the low-energy physics is determined by perfect insulating fixed point with electrons backscattering.

2.1.2. Differential conductance

In what follows, we calculate the low energy physical observable conductance of our setup for $K < 1$ with physical interest. For convenience, the TSC, leads

Table 1: Phase diagram for the point tunneling junction of 1D TSC and integer TI

Region	Fixed point
$K > \sqrt{3}$	perfect Andreev reflection
$1/2 < K < \sqrt{3}$	$A \otimes N$ or $N \otimes A$
$K < 1/2$	perfect insulating

L_μ and R_μ (the left and right sides for the edge of TI) are labeled as 0, 1, and 2. For the $K < 1/2$, the leading irrelevant scattering processes are electron transmission and Majorana fermion tunneling. The tunneling conductance G between TSC and TI, and conductance G_{12} between leads L_μ and R_μ to the lowest-order approximation in infinitesimal voltage V or temperature T are

$$G(V) \sim V^{1/K-2}, G(T) \sim T^{1/K-2}, \quad (16)$$

$$G_{12}(V) \sim V^{2/K-2}, G_{12}(T) \sim T^{2/K-2}. \quad (17)$$

For the $1/2 < K < 1$, we assume first that the system flows toward $A \otimes N$ fixed point and then calculate the differential conductance. The results for $N \otimes A$ fixed point are straightforward. Now, the perfect Andreev reflection occurs at the left side and perfect normal reflection occurs at the right side. The conductance G_{01} between TSC and lead L_μ , conductance G_{02} between TSC and lead R_μ , and conductance G_{12} between leads L_μ and R_μ in bias voltage V are

$$G_{01}(V) \sim \left(\frac{2e^2}{h} - c_V V^{4K-2} \right), \quad (18)$$

$$G_{02}(V) \sim V^{4/K-2}, \quad (19)$$

$$G_{12}(V) \sim V^{K+1/K-2}, \quad (20)$$

where c_V is a non-universal constant. The low temperature dependences of these conductance have similar power-law scaling behaviors.

When the 1D TSC is in topological trivial phase and Majorana fermion tunneling is absent, the tunneling conductance between TSC and 2D TI, and conductance G_{12} between leads L_μ and R_μ for $K < 1$ are

$$G(V) \sim V^{4/K-2}, G(T) \sim T^{4/K-2} \quad (21)$$

$$G_{12}(V) \sim V^{2/K-2}, G_{12}(T) \sim T^{2/K-2} \quad (22)$$

where the Cooper-pair tunneling and electrons transmission terms are the leading irrelevant operators.

Finally, we discuss the experimental measurements for our setup. The experimental evidences of TSC have been shown in InSb quantum wire[15, 16, 17]. On the other hand, the 2D TI has been observed in HgTe/CdTe[58] and InAs/GaSb[59] quantum wells. Here, we take the HgTe/CdTe for example. It is rather nontrivial to estimate the experimentally edge interaction parameter K of 2D TI. As calculated in Refs. [60] and [61], the value of interaction parameter

for HgTe/CdTe quantum well is $0.5 < K < 0.55$. So, in the case of HgTe/CdTe quantum well, the low-energy physics is determined by the non-trivial stable $A \otimes N$ or $N \otimes A$ fixed points. The different bias voltage dependences in Eqs. (18-22) can identify whether the TSC is nontrivial or not. So, the quantized conductance and different power-law scaling behaviors in Eqs. (18-20) can be used as a signature for the Majorana fermion in 1D TSC. For the InAs/GaSb quantum well, the Fermi velocity of the edge modes can be controlled by gates and Luttinger interacting parameter can be fine tuned[62], we can use the InAs/GaSb quantum well to test the phase diagram of integer TI coupling to 1D TSC as a function of the Luttinger interacting parameter.

2.2. Fractional topological insulator case

From the Eqs. (12-14), we can see that for all odd integer $m > 1$, the tunneling term t of Majorana fermion coupling to electrons is irrelevant. When $K > m$, the Cooper-pair tunneling term Δ is relevant and the low-energy transport is controlled by perfect Andreev reflection fixed point with quantized zero-bias conductance $2e^2/h$. When $1/m < K < m$, the low-energy physics is governed by the perfect normal reflection fixed point with a vanishing zero-bias tunneling conductance. For $K < 1/m$, the electrons backscattering is relevant and the system flows to the perfect insulating fixed point at low energies. This fixed point corresponds to the physics picture where the backscattering cuts the edge into two halves and the conductance between the leads μ_1 and μ_2 is zero.

Now we analyze the stability of the perfect insulating fixed point. There are three types of scattering processes that might destabilize the fixed point: Majorana fermion tunneling, Cooper-pair tunneling, and the quasiparticles $\psi_{R/L,\alpha}(x) = F_\alpha e^{i\phi_\alpha(x)}$ (F_α is the Klein factor) transmission. The same RG analysis also applies to this perfect insulating fixed point. The scaling dimensions of quasiparticles transmission, Majorana fermion coupling, and Cooper-pair tunneling are given by $1/(mK)$, $m/(2K)$, and $2m/K$. We can see that for $K < 1/m$, these three processes are all irrelevant and this fixed point is stable for strong repulsive interaction. Next, we calculate the corrections to the tunneling conductance G and two-terminal conductance G_{12} between leads L_μ and R_μ due to finite bias voltage or temperature. The scaling behaviors of the tunneling conductance G and two-terminal conductance G_{12} to the lowest-order approximation are

$$G(V) \sim V^{m/K-2}, G(T) \sim T^{m/K-2} \quad (23)$$

$$G_{12}(V) \sim V^{2/mK-2}, G_{12}(T) \sim T^{2/mK-2} \quad (24)$$

In the perfect normal reflection regime, when $\sqrt{3} < K < m$, the leading irrelevant operator around this point is Cooper-pair tunneling term Δ . The tunneling conductance G at bias voltage V (low temperature T) has the power-law form

$$G(V) \sim V^{2m/K-2}, G(T) \sim T^{2m/K-2} \quad (25)$$

and when $1/m < K < \sqrt{3}$, the leading irrelevant operator is Majorana fermion tunneling term and the tunneling conductance G is given by

$$G(V) \sim V^{m(K+1/K)/2-2}, G(T) \sim T^{m(K+1/K)/2-2} \quad (26)$$

The Majorana fermion-induced tunneling is irrelevant which can be rooted in strong repulsive interaction of fractional TI. The quasiparticles of fractional TI have fractional charge and obey fractional exchange statistics which are forbidden for tunneling. In a word, the universal low-energy transport properties is described by perfect Andreev reflection fixed point for $K > m$, perfect normal reflection fixed point for $1/m < K < m$, perfect insulating fixed point for $K < 1/m$. When the 1D TSC is trivial, we can derive the same phase diagram. But, the tunneling conductance has different power-law behaviors when the bias voltage or temperature is nonzero. The power-law form of tunneling conductance G for perfect insulating regime ($K < 1/m$) is

$$G(V) \sim V^{4m/K-2}, G(T) \sim T^{4m/K-2} \quad (27)$$

In the perfect normal reflection regime ($1/m < K < m$), the tunneling conductance G is

$$G(V) \sim V^{2m/K-2}, G(T) \sim T^{2m/K-2} \quad (28)$$

3. Conclusion

In this paper, we have studied the point contact tunneling junction between 1D TSC and integer (fractional) TI with bosonization and renormalization group methods. For the junction of 1D TSC and topological insulator, according to the strength of edge interaction parameter, there is a non-trivial stable fixed point that the edge is cut into two halves, the perfect normal reflection occurs in one side, and perfect Andreev reflection occurs in the other side. We can use the InSb quantum wire and HgTe/CdTe quantum well to test this non-trivial stable fixed point, which can be used to identify the Majorana fermion in 1D TSC. The $A \otimes N$ ($N \otimes A$) and perfect insulating fixed points appear in the setups of Refs. [24] and [28] respectively, however, the edge states of the TI are topologically protected. For the fractional TI case, the universal low-energy transport properties are described by perfect normal reflection, perfect insulating, or perfect Andreev reflection fixed points dependent on the filling fraction and edge interaction parameter of fractional TI. From the above results, we found that there are different fixed points for the different topological matters coupling to TSC. When other strongly correlated topological matters couple with TSC, the exotic electron tunneling transport properties and critical points maybe occur.

Acknowledgment This work was supported by the National Natural Science Foundation of China under grant numbers 11447008 (Z.Z.W.), 11204066 (D.W.K.) 11404095 (Z.W.W.).

References

- [1] S. R. Elliott, M. Franz, *Colloquium : Majorana fermions in nuclear, particle, and solid-state physics*, Rev. Mod. Phys. 87 (2015) 137–163.

- [2] J. Alicea, [New directions in the pursuit of Majorana fermions in solid state systems](#), Rep. Prog. Phys. 75 (2012) 076501.
- [3] C. W. J. Beenakker, [Search for Majorana fermions in superconductors](#), Annu. Rev. Condens. Matter Phys. 4 (2013) 113–136.
- [4] C. Nayak, S. H. Simon, A. Stern, M. Freedman, S. Das Sarma, [Non-abelian anyons and topological quantum computation](#), Rev. Mod. Phys. 80 (2008) 1083–1159.
- [5] L. Fu, C. L. Kane, [Superconducting proximity effect and Majorana fermions at the surface of a topological insulator](#), Phys. Rev. Lett. 100 (2008) 096407.
- [6] L. Fu, C. L. Kane, [Josephson current and noise at a superconductor/quantum-spin-Hall-insulator/superconductor junction](#), Phys. Rev. B 79 (2009) 161408.
- [7] Y. Oreg, G. Refael, F. von Oppen, [Helical liquids and Majorana bound states in quantum wires](#), Phys. Rev. Lett. 105 (2010) 177002.
- [8] R. M. Lutchyn, J. D. Sau, S. Das Sarma, [Majorana fermions and a topological phase transition in semiconductor-superconductor heterostructures](#), Phys. Rev. Lett. 105 (2010) 077001.
- [9] S. Nadj-Perge, I. K. Drozdov, B. A. Bernevig, A. Yazdani, [Proposal for realizing Majorana fermions in chains of magnetic atoms on a superconductor](#), Phys. Rev. B 88 (2013) 020407.
- [10] F. Pientka, L. I. Glazman, F. von Oppen, [Topological superconducting phase in helical Shiba chains](#), Phys. Rev. B 88 (2013) 155420.
- [11] J. Klinovaja, P. Stano, A. Yazdani, D. Loss, [Topological superconductivity and Majorana fermions in RKKY systems](#), Phys. Rev. Lett. 111 (2013) 186805.
- [12] B. Braunecker, P. Simon, [Interplay between classical magnetic moments and superconductivity in quantum one-dimensional conductors: Toward a self-sustained topological Majorana phase](#), Phys. Rev. Lett. 111 (2013) 147202.
- [13] M. M. Vazifeh, M. Franz, [Self-organized topological state with Majorana fermions](#), Phys. Rev. Lett. 111 (2013) 206802.
- [14] T. D. Stanescu, S. Tewari, [Majorana fermions in semiconductor nanowires: fundamentals, modeling, and experiment](#), J. Phys.: Condens. Matter 25 (2013) 233201.
- [15] V. Mourik, K. Zuo, S. M. Frolov, S. R. Plissard, E. P. A. M. Bakkers, L. P. Kouwenhoven, [Signatures of Majorana fermions in hybrid superconductor-semiconductor nanowire devices](#), Science 336 (2012) 1003–1007.

- [16] A. Das, Y. Ronen, Y. Most, Y. Oreg, M. Heiblum, H. Shtrikman, [Zero-bias peaks and splitting in an al-inas nanowire topological superconductor as a signature of Majorana fermions](#), *Nature Phys.* 8 (2012) 887–895.
- [17] M. T. Deng, C. L. Yu, G. Y. Huang, M. Larsson, P. Caroff, H. Q. Xu, [Anomalous zero-bias conductance peak in a Nb-InSb nanowire-Nb hybrid device](#), *Nano Lett.* 12 (2012) 6414–6419.
- [18] S. Hart, H. Ren, T. Wagner, P. Leubner, M. Mhlbauer, C. Brne, H. Buhmann, L. W. Molenkamp, A. Yacoby, [Induced superconductivity in the quantum spin Hall edge](#), *Nature Phys.* 10 (2014) 638–643.
- [19] S. Nadj-Perge, I. K. Drozdov, J. Li, H. Chen, S. Jeon, J. Seo, A. H. MacDonald, B. A. Bernevig, A. Yazdani, [Observation of Majorana fermions in ferromagnetic atomic chains on a superconductor](#), *Science* 346 (2014) 602–607.
- [20] K. T. Law, P. A. Lee, T. K. Ng, [Majorana fermion induced resonant Andreev reflection](#), *Phys. Rev. Lett.* 103 (2009) 237001.
- [21] A. Zazunov, A. L. Yeyati, R. Egger, [Coulomb blockade of Majorana-fermion-induced transport](#), *Phys. Rev. B* 84 (2011) 165440.
- [22] R. Hütten, A. Zazunov, B. Braunecker, A. L. Yeyati, R. Egger, [Majorana single-charge transistor](#), *Phys. Rev. Lett.* 109 (2012) 166403.
- [23] L. Fidkowski, J. Alicea, N. H. Lindner, R. M. Lutchyn, M. P. A. Fisher, [Universal transport signatures of Majorana fermions in superconductor-Luttinger liquid junctions](#), *Phys. Rev. B* 85 (2012) 245121.
- [24] I. Affleck, D. Giuliano, [Topological superconductor-Luttinger liquid junctions](#), *J. Stat. Mech.* 2013 (2013) P06011.
- [25] Y. Komijani, I. Affleck, [Detecting a quantum critical point in topological SN junctions](#), *Phys. Rev. B* 90 (2014) 115107.
- [26] R. M. Lutchyn, J. H. Skrabacz, [Transport properties of topological superconductor-Luttinger liquid junctions: A real-time keldysh approach](#), *Phys. Rev. B* 88 (2013) 024511.
- [27] R. Vasseur, J. P. Dahlhaus, J. E. Moore, [Universal nonequilibrium signatures of Majorana zero modes in quench dynamics](#), *Phys. Rev. X* 4 (2014) 041007.
- [28] Y.-W. Lee, Y.-L. Lee, [Tunneling between a topological superconductor and a Luttinger liquid](#), *Phys. Rev. B* 89 (2014) 125417.
- [29] A. Zazunov, A. Altland, R. Egger, [Transport properties of the Coulomb-Majorana junction](#), *New J. Phys.* 16 (2014) 015010.

- [30] A. Altland, B. Béri, R. Egger, A. M. Tsvelik, [Multichannel Kondo impurity dynamics in a Majorana device](#), Phys. Rev. Lett. 113 (2014) 076401.
- [31] E. Eriksson, C. Mora, A. Zazunov, R. Egger, [Non-fermi-liquid manifold in a Majorana device](#), Phys. Rev. Lett. 113 (2014) 076404.
- [32] S.-P. Chao, T. L. Schmidt, C.-H. Chung, [Tunneling between helical Majorana modes and helical Luttinger liquids](#), Phys. Rev. B 91 (2015) 235125.
- [33] D. I. Pikulin, Y. Komijani, I. Affleck, [Luttinger liquid in contact with a kramers pair of Majorana bound states](#), Phys. Rev. B. 93 (2016) 205430.
- [34] A. O. Gogolin, A. A. Nersesyan, A. M. Tsvelik, [Bosonization and strongly correlated systems](#), Cambridge Univ. Press, 1998.
- [35] T. Giamarchi, [Quantum physics in one dimension](#), Oxford Univ. Press, 2004.
- [36] Z. W. Zuo, H. Li, L. B. Li, L. Sheng, R. Shen, D. Y. Xing, [Detecting Majorana fermions by use of superconductor-quantum Hall liquid junctions](#), Europhys. Lett. 114 (2016) 27001.
- [37] C. Benjamin, J. K. Pachos, [Detecting Majorana bound states](#), Phys. Rev. B 81 (2010) 085101.
- [38] B. A. Bernevig, S.-C. Zhang, [Quantum spin Hall effect](#), Phys. Rev. Lett. 96 (2006) 106802.
- [39] M. Levin, A. Stern, [Fractional topological insulators](#), Phys. Rev. Lett. 103 (2009) 196803.
- [40] T. Neupert, L. Santos, S. Ryu, C. Chamon, C. Mudry, [Fractional topological liquids with time-reversal symmetry and their lattice realization](#), Phys. Rev. B 84 (2011) 165107.
- [41] T. Neupert, C. Chamon, T. Iadecola, L. H. Santos, C. Mudry, [Fractional \(Chern and topological\) insulators](#), Phys. Scr. T164 (2015) 014005.
- [42] J. Maciejko, G. A. Fiete, [Fractionalized topological insulators](#), Nature Phys. 11 (2015) 385–388.
- [43] A. Stern, [Fractional topological insulators - a pedagogical review](#), Annu. Rev. Condens. Matter Phys. 7 (2016) 349–368.
- [44] D. J. Clarke, J. Alicea, K. Shtengel, [Exotic non-abelian anyons from conventional fractional quantum Hall states](#), Nature Commun. 4 (2013) 1348.
- [45] N. H. Lindner, E. Berg, G. Refael, A. Stern, [Fractionalizing Majorana fermions: Non-abelian statistics on the edges of abelian quantum Hall states](#), Phys. Rev. X 2 (2012) 041002.

- [46] M. Cheng, [Superconducting proximity effect on the edge of fractional topological insulators](#), Phys. Rev. B 86 (2012) 195126.
- [47] A. Vaezi, [Fractional topological superconductor with fractionalized Majorana fermions](#), Phys. Rev. B 87 (2013) 035132.
- [48] C. Wu, B. A. Bernevig, S.-C. Zhang, [Helical liquid and the edge of quantum spin Hall systems](#), Phys. Rev. Lett. 96 (2006) 106401.
- [49] C. Xu, J. E. Moore, [Stability of the quantum spin Hall effect: Effects of interactions, disorder, and Z2 topology](#), Phys. Rev. B 73 (2006) 045322.
- [50] B. Béri, N. R. Cooper, [Probing fractional topological insulators with magnetic edge perturbations](#), Phys. Rev. Lett. 108 (2012) 206804.
- [51] B. Béri, [Majorana-Klein hybridization in topological superconductor junctions](#), Phys. Rev. Lett. 110 (2013) 216803.
- [52] A. Altland, R. Egger, [Multiterminal Coulomb-Majorana junction](#), Phys. Rev. Lett. 110 (2013) 196401.
- [53] J. Alicea, Y. Oreg, G. Refael, F. Von Oppen, M. P. Fisher, [Non-abelian statistics and topological quantum information processing in 1d wire networks](#), Nature Phys. 7 (2011) 412–417.
- [54] E.-A. Kim, S. Vishveshwara, E. Fradkin, [Cooper-pair tunneling in junctions of singlet quantum Hall states and superconductors](#), Phys. Rev. Lett. 93 (2004) 266803.
- [55] Z. W. Zuo, L. Sheng, D. Y. Xing, [Crossed andreev reflections in superconductor and fractional quantum Hall liquids hybrid system](#), Solid State Commun. 184 (2014) 17–20.
- [56] D. Sticlet, C. Bena, P. Simon, [Spin and Majorana polarization in topological superconducting wires](#), Phys. Rev. Lett. 108 (2012) 096802.
- [57] N. Sedlmayr, C. Bena, [Visualizing Majorana bound states in one and two dimensions using the generalized Majorana polarization](#), Phys. Rev. B 92 (2015) 115115.
- [58] M. König, S. Wiedmann, C. Brüne, A. Roth, H. Buhmann, L. W. Molenkamp, X.-L. Qi, S.-C. Zhang, [Quantum spin Hall insulator state in HgTe quantum wells](#), Science 318 (2007) 766–770.
- [59] I. Knez, R.-R. Du, G. Sullivan, [Evidence for helical edge modes in inverted InAs/GaSb quantum wells](#), Phys. Rev. Lett. 107 (2011) 136603.
- [60] C.-Y. Hou, E.-A. Kim, C. Chamon, [Corner junction as a probe of helical edge states](#), Phys. Rev. Lett. 102 (2009) 076602.

- [61] A. Ström, H. Johannesson, G. I. Japaridze, [Edge dynamics in a quantum spin Hall state: Effects from Rashba spin-orbit interaction](#), Phys. Rev. Lett. 104 (2010) 256804.
- [62] T. Li, P. Wang, H. Fu, L. Du, K. A. Schreiber, X. Mu, X. Liu, G. Sullivan, G. A. Csáthy, X. Lin, R.-R. Du, [Observation of a helical Luttinger liquid in InAs/GaSb quantum spin Hall edges](#), Phys. Rev. Lett. 115 (2015) 136804.